Copyright Warning & Restrictions

The copyright law of the United States (Title 17, United States Code) governs the making of photocopies or other reproductions of copyrighted material.

Under certain conditions specified in the law, libraries and archives are authorized to furnish a photocopy or other reproduction. One of these specified conditions is that the photocopy or reproduction is not to be "used for any purpose other than private study, scholarship, or research." If a, user makes a request for, or later uses, a photocopy or reproduction for purposes in excess of "fair use" that user may be liable for copyright infringement,

This institution reserves the right to refuse to accept a copying order if, in its judgment, fulfillment of the order would involve violation of copyright law.

Please Note: The author retains the copyright while the New Jersey Institute of Technology reserves the right to distribute this thesis or dissertation

Printing note: If you do not wish to print this page, then select "Pages from: first page # to: last page #" on the print dialog screen

ABSTRACT

SYNTHESIS OF BORON NITRIDE/VYCOR COMPOSITE MEMBRANE STRUCTURES BY AN OPTIMIZED LPCVD PROCESS

by
Chenna Ravindranath

Since the advent of the idea of ultrafiltration , microporous membranes have come through a long way in establishing a niche as an efficient technology for gas separation applications. More and more research is aimed at reducing pore size towards nanolevels, when separation factor is the criterion rather than the permeability. This work is focused at synthesizing and characterizing microporous inorganic membranes for gas separations by molecular sieving. BN was deposited on mesoporous vycor tubes using triethylamine borane complex (TEAB) and ammonia as precursors. Effect of temperature and deposition geometry on permeability of various gases has been studied. Very high selectivities have been achieved for separation of small inorganic gases such as He, H_2 from N_2. Activation energy study indicate that the permeability of He and H_2 are thermally activated with activation energies of 39.7 kJ/mol and 50kJ/mol respectively. XRD analysis indicate an amorphous BN deposit in the vycor tube.

SYNTHESIS OF
BORON NITRIDE/ VYCOR COMPOSITE MEMBRANE STRUCTURES
BY AN OPTIMIZED LPCVD PROCESS

by
Chenna Ravindranath

A Thesis
Submitted to the Faculty of
New Jersey Institute of Technology
in Partial Fulfillment of the Requirements for the Degree of
Master of Science in Engineering Science

Interdisciplinary Program in Materials Science and Engineering

October 1995

APPROVAL PAGE

SYNTHESIS OF
BORON NITRIDE/VYCOR COMPOSITE MEMBRANE STRUCTURES
BY AN OPTIMIZED LPCVD PROCESS

Chenna Ravindranath

Dr. Roland A. Levy, Thesis Advisor — Date
Professor of Physics,
Director of Materials Science and Engineering Program, NJIT

Dr. Lev N. Krasnoperov, Thesis Advisor — Date
Professor of Chemical Engineering, Chemistry, and
Environmental Science, NJIT

Dr. James M. Grow — Date
Professor of Chemical Engineering, Chemistry, and
Environmental Science, NJIT.

BIOGRAPHICAL SKETCH

Author: Chenna Ravindranath

Degree: Master of Science in Engineering Science

Date: October, 1995

Undergraduate and Graduate Education:

- Master of Science in Engineering Science,
  New Jersey Institute of Technology,
  Newark, New Jersey, 1995

- Bachelor Engineering in Metallurgy
  Karnataka Regional Engineering College
  Karnataka, India, 1994

Major: Materials Science and Engineering

This thesis is dedicated to
my parents

ACKNOWLEDGMENT

The author express his sincere gratitude to his advisors, Professor Roland A. Levy and Professor Lev N. Krasnoperov for their guidance, inspiration, and support throughout this research.

Special thanks to Professor James M. Grow for serving as a member of the committee.

The author appreciates the timely help and suggestions from Dr. Jan Opyrchal and Emmanuel Ramos and other CVD laboratory members including: Vitaly Sigal, Romiana Petrova, Venkat Paturi, Mahalingam Bhaskaran, Hong Yu Chen, Lan Chen, David Perese, Manish Narayan and Majda Newman.

TABLE OF CONTENTS

TABLE OF CONTENTS
(Continued)

TABLE OF CONTENTS
(Continued)

LIST OF TABLES

LIST OF FIGURES

CHAPTER 1

INTRODUCTION

1.1 Growth of Ceramic Membranes

Historically , the progress of civilization has been earmarked by the ability to separate and recombine materials and matter. Ability to separate various metals at various periods led to the evolution of the Bronze Age and the Iron Age. Current work in the area of separation of molecules and atoms will immensely improve the quality of life in the coming years. It is in this realm of separation technology that microporous ceramic membranes have gained considerable interest and the improvements in their synthesis have been at a tremendous pace.

The past has seen the increasing use of polymeric membranes[1] for separation of mixtures in process industries such as desalination, food and beverage, and waste water treatment. Extensive studies have been made and are still being made on the properties and application of polymeric membranes[2,3]. Polymeric membranes exhibit excellent selectivity, and stability towards hostile environment. Moreover, the pore sizes and their distribution can be tailored to obtain the desired properties. In spite of their advantages and the constant research going on to improve their properties they have not been able to meet the demands for high temperature applications. One of the main reasons for this is the fact that polymers, being organic compounds[4] with weak bonds,

are highly unstable at high temperatures and soften to such an extent that they collapse under their own weight. It is because of this fact that ceramic membranes have attracted scientific interest for so long.

Ten years ago, the ceramic membranes employed for gas separations were typically based on the use of Knudsen diffusion as the primary mechanism of transport. However, currently available ceramic membrane technology allows one to utilize not only Knudsen diffusion but also surface activated transport as vehicles for bringing about molecular separations. Table 1.1 gives a list of some of the currently available inorganic ceramic membranes.

Table 1-1 Commercial ceramic membranes

Manufacturer	**Membrane material**	**Diameter of pores in the membrane**
US Filter	ZrO_2	200Å
US Filter	Al_2O_3	50Å
Alcan/Anotec	Al_2O_3	200Å
Gaston county Filtration systems	Zro_2	40Å
Rhone-Poulene/SFEC	ZrO_2	40Å
TDK	ZrO_2	~100Å
Schott Glass	Glass	100Å
Fuji Filters	Glass	40Å

1.2 Advantages of Ceramic Membranes

The following are the advantages of ceramic membranes over polymer membranes:

- High temperature applications[5]: Ceramics are outstanding when it comes to high temperatures and are in fact stable even at temperatures as high as 1000°C[6].
- Inertness: Their resistance to chemicals makes them virtually immune to a wide variety of solvents, acids, alkalines, and detergents.
- Strength: Polymeric membranes are typically cast by polymerization processes and hence are made up of networks of chains whereas ceramic membranes are made by starting with assemblies of crystals and particles. As a result of the compact crystal structure, chemical bonding and high field strengths associated with the small and highly charged cations, ceramic membranes have very good structural integrity. This feature allows them to be used at very high pressures (30 atm) concatenated by high throughput. This leads to more efficient energy usage especially for processes in which fouling is a big problem.
- Cost economics[1]: In the competitive arena of technologies or materials, cost economics is undoubtedly a key selection factor. Because ceramic membranes have the capacity of providing extremely high filtration surface area, they should be able to provide great economy-of-scale and therefore, very cost-competitive operations. Moreover their structural integrity permits

high-pressure operation and high-throughput production, further driving the costs down.

1.3 Materials and Applications

Usually ceramic membranes are not free standing. Instead they are deposited onto a substrate which has a larger mean pore size. This substrate should possess some basic properties for the efficient performance of the membranes. The basic requirements for membrane support are[7],

1. Ability to maintain structural/mechanical integrity over a wide range of temperatures and pressures.
2. Large surface areas with mesopores providing high inherent permeabilities
3. Narrow pore size distribution
4. Pin hole, microcrack and defect free structures
5. Ability to withstand property degradation in corrosive environments
6. And finally the difference between the coefficients of thermal expansion for the support and the deposit should be as low as possible to reduce the possibility of microcrack formation in the membranes, the primary source of membrane failures.

The substrate used in our study was a porous Vycor tube manufactured by Corning Inc., and is commercially available as Vycor 7930. Vycor glass is made up of 94-95% SiO_2, the rest being Na_2O. Processing of the substrate is discussed in the next chapter.

There are approximately nine major types of ceramics used for the manufacture of ceramic membranes: Alumina, borosilicate, cordierite, mullite, silicon carbide, silicon nitride, zirconia, silica and titania. These membranes usually come in three configurations: hollow fibers, flat plates, and honeycombs. The following are the areas where ceramic membranes have set their mark:

- gas separation: involves mainly the removal of hydrogen from refinery stream, and carbon dioxide and hydrogen sulfide from natural gas.
- biotechnology/pharmaceutical: Removal of viruses from culture broth and purification of amino acids, vitamins, and organic acids.
- petrochemical: catalytic dehydrogenation[8] of large molecules at low temperatures and also used for coal gasification
- environmental control: To get rid of precipitated radionuclides and metaloxides.
- concentration and homogenization of milk and eggs.
- metal refining: removal of impurities and undesirable metal oxides from superalloys.

Innovative applications are still being discovered such as an integrated membrane[9]. This composite membrane consists of a selective layer and a catalytic layer. The selective layer allows the migration of only the reactant and blocks the impurities. The reactant then comes in contact with the catalytic layer where it is converted into the product and is subsequently swept off by convective forces. The benefits of such a process are highly simplified

processing, no byproducts and faster kinetics. A prototype has been developed for use in hydrocarbon oxidation and hydrogenation processes.

1.4 BN as a Membrane Layer

The reason for selecting BN as the membrane layer was due to a an ongoing project involving deposition of BN on Si wafers. BN thin films were obtained using the same setup and precursors. The work showed that excellent films of BN could be deposited using TEAB and NH_3. BN thus deposited was found to be stable when exposed to atmosphere for a long time. The films also had a slight compressive stress below a deposition temperature of 325°C and had very little carbon content. The effect of NH_3 was found to lower the deposition temperature down to 300°C.

Also BN[10,11] has some very attractive inherent properties which make it a potential competitor as a membrane material. BN is not attacked by mineral acids and, in general, has been found to be very resistant to other chemical attacks. It starts dissociating at 2700°C in vacuum and is oxidized[12] in air only at temperatures as high as 1200°C.

1.5 TEAB as a Precursor

Extensive work has been done on the chemical vapor deposition[13] of BN thin films on various substrates including silicon, quartz, and glass. A wide range of precursors have been used to obtain these thin films which include diborane[14],

borontrichloride[15], triethyl boron[16], decarborane[17] and boron triethylamine complex. This study indicates that TEAB has several advantages over many of the other precursors.

TEAB is a relatively non-toxic and non explosive substance and this obviates the need for expensive cabinets and a cross purging gas supply for safety reasons. However, TEAB has a low vapor pressure and hence has to be forced into the reactor under high pressure. The properties of TEAB are given in Table 1-2[18].

Table 1-2 Properties of TEAB

Chemical name	Borane triethylamine complex (TEAB)
Chemical formula	$(C_2H_5)_3N.BH_3$
Molecular weight (g/mol)	115.03
Specific gravity (g/cc)	0.777
Freezing Point	-3°C
Boiling point	100°C
Appearance	Colorless liquid
Vapor pressure	~ 20 mTorr
CAS Registry number	1722-26-5

CHAPTER 2

METHODS FOR MEMBRANE SYNTHESIS

Various methods have been developed for the synthesis of membranes which include sol-gel technique, deposition process, leaching, controlled pyrolysis, Anodic oxidation etc., However only those methods which are widely practiced are discussed.

2.1 Sol-Gel Technique

This process has been so successful that it has been commercially utilized to obtain membranes. It is multistage in nature involving many stages before the ultimate product can be obtained.

Sol contains fine hydrated oxide particles of sub-micron size. These particles are formed from polymerization of metal alkoxides. Sol-Gel[19,20] method involves preparation of a suitable sol based on the type of membrane required, gelation of the sol to obtain a solid deposit and then firing at elevated temperatures until the deposit is firmly attached to the support. Each step has to be controlled precisely since they in turn affect the properties of the final membrane.

The size of the particles in the sol strongly determines the size of the final pore and can be tailored by changing the pH of the medium, the molar ratios of alkoxides, temperature, feed rate of the reactants etc., The particles have to be

alkoxides, temperature, feed rate of the reactants etc., The particles have to be uniformly[21] distributed in the medium to obviate any non-uniform deposit. Also, the particles have to behave individually rather than act together as an agglomerate. For this purpose stabilizing or deagglomerating agents such as aliphatic acids, or bases are added to control the pH of the sol and thus inducing surface charge on the particles.

The sol is then applied to the support either by dipping the support in the sol or by slip casting. Gelation involves the aggregation of particles when the solvent is evaporated. The most important factor here is the rate of evaporation which can be controlled by conventional means.

The final stage is the firing of the gelled sol along with the support. A thorough understanding of the phase changes and thermal/hydrodynamic stresses developed during firing is essential to hold the membrane to the support.

Sol gel technique is extensively used for Alumina, Zirconia and Titania membranes. One of the main limitations of this technique is that the pore size is strongly dependent on the particles size which cannot be obtained accurately. The final pore sizes rarely cross below the 40Å diameter and hence are useful for ultrafiltration. Research in this field is aimed mainly at obtaining finer particles with diameter around 30Å.

2.2 Electroless Plating

The mechanism of separation of gaseous mixtures using membranes synthesized by this method is different from porous ceramic membranes. The principle involves the adsorption of gas molecules, solution in the metal film and subsequent interdiffusion in the metal. Separation occurs depending upon the extent of solution of the individual gases in the metal film. Hydrogen has higher solubility than nitrogen and a separation factor of 1000-5000 has been obtained.

This technique has been used to obtain metal deposits on various substrates. Basically metallic membranes are dense non-porous membranes. A composite palladium-ceramic membrane has been obtained by Collins[22]. Electroless plating[22] involves the deposition of metal films with or without the aid of voltage potential. The vycor tube, to be coated, is dipped in a suitable bath containing metal complex and stabilizer or reducing agents as required.

This method has many disadvantages. First the vycor tube has to undergo several pretreatment steps and a surface activation step prior to plating. The tube has to be cleaned by ultrasonic rinsing in an alkaline solution, deionized water and isopropylalcohol to remove sand and grit from the membrane. The surface activation step is done to seed the inner membrane with finely divided palladium nuclei to initiate the process. This step is important to obtain defect free palladium films. Surface activation is done by immersing the vycor in a suitable solution until a uniform activated membrane is achieved. Additionally, metallic films are relatively unstable at high temperatures because

of interdiffusion and the probability of oxidation in corrosive media. Interdiffusion occurs when more than one different layer is deposited and which has to be overcome by placing a barrier between the layers.

2.3 Acid Leaching

This method[23] is based on the fact that some of the glasses separate into two phases upon heat treatment. Turner and Winks[24] first published a paper in 1926 on the leaching of glasses containing boric oxide using hydrochloric acid.

Leaching has been done predominantly on alkali boro silicate glasses. Glass is first subjected to heat treatment wherein at high temperatures two phases separate out. One phase is almost pure silica while the other is rich in Na_2O and B_2O_3. As the temperature is lowered, a tendency to form Na-O-B bonds rather than Na-O-Si bonds is developed. Simultaneous separation proceeds into an insoluble phase(-Si-O-Si-) and a soluble phase(-Na-O-B-)[25]. The latter phase is then leached by either an acid or a base or just water.

Acid leaching is a complicated process and extreme care has to be taken to obtain defect free porous glass. A strain is set up, partly from purely physical causes, because of capillary forces developing in the pores due to the presence of acid. The strain can be induced either by *swelling* of the leached layer or by *shrinking*. Glass is then scrubbed with water and dried slowly to remove excess water.

The porous vycor glass thus obtained has a pore diameter ranging from 20 - 40Å and with a porosity of about 30%. Porous vycor glass can absorb atmospheric moisture by as much as 25% of its own weight. These glasses are commercially available as Vycor No.7930.

2.4 Deposition Methods

These methods only modifiy existing large pores down to a size which is favorable for separation. Hence, a porous substrate is required, which is free of defects such as cracks or pinholes. Compounds or elements are deposited inside the pores and thus narrowing down the pore size. Deposition methods can be classified under two groups namely, Physical Vapor Deposition (PVD) and Chemical Vapor Deposition (CVD). For the sake of convenience CVD is discussed in detail in the next section. However, a variation of CVD is discussed here.

2.4.1 Physical Vapor Deposition

PVD[26] involves deposition of material onto a substrate without any chemical reaction at the surface. The two most important methods under PVD are Evaporation and Sputtering.

In evaporation, atoms are removed from the source by thermal means, whereas in sputtering the atoms are dislodged from the target by the impact of

gaseous ions. PVD gained considerable importance due to improvements in vacuum pumping equipment as well as in the heating sources.

In general, the properties of the film obtained by PVD are governed by the following:

- evaporation rate of the atoms
- vapor pressure of the target materials
- deposition geometry
- temperature
- pressure
- thermal history of the substrate

The factors that distinguish PVD from CVD are:

- Reliance on solid materials
- Physical mechanisms by which source atoms enter the gas phase
- General absence of chemical reactions

2.4.2 Spray Pyrolysis

Spray pyrolysis[27] (Chemical Spray Deposition) is a low cost process which has recently been utilized to prepare thin polycrystalline films of a wide variety of compound semiconductors[28]. Spray pyrolysis of binary semiconductors invokes the spraying of an aqueous solution containing soluble salts of the constituent atoms onto a heated substrate. The parameters that control the process are

spray rates and temperature of the substrate. Films made of CdS have been prepared from a solution containing $CdCl_2$ and NH_2CSNH_2 (thiourea).

2.5 Chemical Vapor Deposition

Chemical Vapor Deposition is a well known method for the manufacture of films in silicon integrated circuits. A very large variety of materials can be formed by this method. A major advantage of this method over similar competing processes is that the materials can be deposited at relatively lower temperatures by using plasma enhanced CVD.techniques This is an important fact since the interdiffusion of elements in integrated circuits caused by high temperatures is highly undesirable. Low temperatures are also desired in view of the facts such as material warpage due to the stresses developed, crystallographic damage and contamination of the deposits can be minimized. Of particular note is the nature of the deposits which can be easily controlled regarding their homogeneity, conformality and composition. Both chemical composition and physical structure can be modified by controlling the reaction chemistry and deposition conditions. Membrane synthesis by CVD[29] has been studied by many researchers.

2.5.1 Basic Aspects of CVD

Chemical Vapor Deposition comprises all those processes wherein the deposit is obtained by a chemical reaction either on or near the substrate surface. The

deposit can be single crystal, polycrystalline or even amorphous. Chemical and physical conditions strongly affect the composition and structure of the film.

A complete study of CVD[26] films involves an in-depth knowledge of areas such as gas phase reaction chemistry, thermodynamics, kinetics, heat transfer, fluid mechanics, catalysis, free radical chemistry, surface reactions, plasma reactions, radiation chemistry, transport mechanisms, film growth phenomena and reactor engineering. As such CVD is a complex process and a thorough understanding of the above aspects becomes of utmost importance.

Deposits can be obtained by several different chemical reactions which include pyrolysis, oxidation, reduction, hydrolysis, nitride and carbide formation, synthesis reactions, and disproportination. Physical properties of the reactants and the products also affect the deposition rate. If the reactants are in liquid phase then high vapor pressures are favorable since they could then be transported into the reaction chamber with the help of carrier gases. Solids are usually melted and treated as liquids. The vapor pressure of side products should also be high to facilitate their removal from the reaction sites, whereas the resulting products should have low volatility. The chemical reactions can be driven either by thermal energy (electric glow discharge or convection) or by electromagnetic radiation (usually ultraviolet or laser radiation). These reactions can be homogeneous or heterogeneous, or a combination of both. Homogeneous reactions occur in the gas phase, away from the substrate and are not desirable. This is because homogeneous reactions result in particulate

deposits with lower density. Heterogeneous reactions on the other hand occur on the substrate and hence are almost void less.

A study of the thermodynamics of the reactions is very important. It gives information about the theoretical feasibility and efficiency of the reaction under specified conditions of temperature and pressure. But the data obtained cannot be taken as the sole criterion since in obtaining this data it is assumed that thermodynamic equilibrium exists inside the reaction chamber.

Commercial success of a process is determined by the rate of productivity, in this case the deposition rate. Chemical kinetics allows the determination of deposition rate. The activation energy derived from Arrhenius plots gives an idea about the rate-controlling step. Two major rate controlling steps are the surface processes and diffusion processes. The surface process is the rate controlling step at low temperatures. This process is characterized by an exponential temperature dependence. At higher temperatures the process is diffusion controlled. Diffusion is less dependent on temperature and has a less steep slope.

Transport phenomena relate to the transport of momentum, energy, and mass. Transport phenomenon plays a vital role in obtaining uniform layers in both composition and thickness. Gas flow in reactors is affected by velocity of flow, temperature and its distribution in the reactor, pressure, system geometry, and physical properties of the gases and vapors.

2.5.2 Process Considerations: (vapor deposition)

The chemical reactions of CVD can be effected in a large variety of ways. A brief discussion of these chemical reactions along with examples is given below.

2.5.2.1 Thermal Decomposition or Pyrolysis: In this type of process the substrate is heated to high temperatures to decompose the precursors and thus deposit the non-volatile compound. Since most of the processes involve high temperatures, these type of reactions are further subclassified as high- and low-temperature processes, as processes using organic or inorganic compounds,and as polar or non-polar compounds. Any reaction occurring below 600°C come under low temperature decomposition and above 600°C are high temperature processes. Compounds such as metal hydrides, carbonyls, and organometallics are used for low-temperature processes. Metal halides, particularly iodides are used in the high temperature regime. However, the compounds used for low temperatures can also used at high temperatures but under conditions of either low pressure or in the presence of gaseous mixtures rich in reaction products. This technique comes in handy when properties such as preferred orientation, crystal structure or size are desired.

2.5.2.2 Hydrogen Reduction: One of the frequently used types of CVD reactions is hydrogen reduction at elevated temperature. The compounds used are metal halides, carbonyl halides or other oxygen containing compounds. In

the latter case, the reducibility of the compound by hydrogen determines the amount of oxide in the deposit. Hydrogen may also be used in other type of reactions where reduction is not the primary objective but to improve the deposit characteristics. Another advantage can be found in the case of metalhydrides. The presence of hydrogen precludes the early decomposition of the hydride and permit the use of higher deposition temperatures.

Hydrogen reaction is carried out at elevated temperatures where the reduction reaction is favored. This temperature may range from about 100°C up to temperatures where the reduction reaction becomes ineffective due to the thermal decomposition of the compound. In this respect hydrogen reaction can be regarded as a thermal decomposition reaction facilitated by removal of one or more of the gaseous products. Consequently the temperature required is lowered by several hundreds degrees. For this reason hydrogen may be used even with easily decomposed compounds to effect a further reduction in the deposition temperature.

It is desirable that the plating compounds have appreciable volatility at temperatures well below the deposition temperature. If this cannot be met, then the compound has to be vaporized by a stream of inert carrier gas and introduced separately into the reaction chamber.

2.5.2.3 Reduction with Metal Vapors: Hydrogen is not always preferable as reducing agent. For example, the hydrogen reduction of metals such as

zirconium, titanium or beryllium from their halides is practically not feasible since hydrogen is a weak reducing agent for these type of metal halides. It is found that metal vapors are much stronger reducing agents than hydrogen. Hence, vapors of zinc and magnesium are used to deposit these metals. In fact zinc vapors have been used to deposit silicon and boron from their halide vapors. The use of zinc results in higher yields of metals and faster deposition rates. Alternatively, metal deposition can be carried out at a feasible rate at much lower temperatures by the use of the stronger reducing agent.

Alkali vapors such as sodium are very strong reducing agents and sometimes introduces the risk of premature reduction in the gas phase. This results in the formation of powdered deposits instead of dense, coherent deposits. Hence the selection of a proper reducing agent is critical in these type of reactions.

The criteria for the selection of these agents is the free energy of formation of their halides. Usually, those metals whose halide has a free energy of formation within ±10 kcal/g-atom of that of the metal halide vapor to be reduced are preferred.

2.5.2.4 Substrate Reaction: Deposition can also take place with the substrate itself entering into a chemical reaction with the reactant gases. There are four ways in which substrate can react.

The substrate can act as a reducing agent for a metal halide vapor and subsequently turning into a halide vapor. The major criteria required is that the substrate halide be highly volatile.

The substrate can also react with the deposit in two ways. It can dissolve the deposit and form either an alloy or a solid solution or it can react exothermically to form a moderate or highly stable compound. The substrate can indirectly affect the reaction chemistry by acting as a catalyst.

2.5.3 Type of Reactors

Various types of reactors have been developed over the years. These have been broadly categorized and described by terms such as high and low temperature, atmospheric and low pressure, cold and hot wall and so on.

Low temperature systems are used in the fabrication of Si bipolar and MOS integrated circuits in the temperature range of 325-450^{0}C. However, high-quality epitaxial films could be obtained only at high temperatures. High temperature coatings are also used in metallurgical coatings. High temperature systems can be further divided into hot-wall and cold-wall types. Hot-wall reactors are tubular in form and heating is accomplished by surrounding the reactor with resistance elements. Low temperature reactors are used extensively for the deposition of Si films. The substrates are placed in thermal contact with SiC susceptors and are then inductively heated, while the walls of the reactor are water or air cooled.

Low pressure CVD or LPCVD was first used to deposit polysilicon films. A gas pressure of ~ 0.5 to 1.0 Torr is employed in LPCVD reactors. To compensate for the low pressure the input gas concentration is increased relative to the atmospheric reactor case. Low gas pressures mainly increase the flux of gases through the boundary layer between the substrate and the gas stream. This in turn is responsible for the higher film growth rates observed in LPCVD systems.

Further, CVD reactors can be either plasma or laser enhanced. In both the cases the energy available is used to decompose the gas molecules into a variety of component species such as electrons, ions, atoms, and molecules. The net effect of the interactions among these fragments is to cause chemical reaction to occur at much lower temperatures than in conventional CVD systems.

CHAPTER 3

CHARACTERIZATION OF MEMBRANES

Several techniques are available to characterize ceramic membranes. The performance of membranes depends largely on the following factors and hence the need to evaluate these parameters arises.

1. Pore size and Pore Distribution
2. Activation energy of gas permeation
3. Stability of the membrane.

3.1 Pore Characterization

In ceramic membranes the flow of gases is largely controlled by the characteristics of the pores and their distribution. Pores can be characterized[30,31] by several methods. The main factor which distinguishes these types is the pore size itself. In other words, the reliability of these various types depends on the pore size of the material that has to be characterized. Other parameters that are important in pore characterization are pore connectivity, porosity and surface area.

Over the years the classification of pores has been undergoing changes to comply with the ever growing knowledge about their sizes and to the extent to

which they could be determined. The following gives an idea of the pore sizes and their classification.

Macropores: greater than 500Å

Mesopores :20Å to 500Å

Micropores :10Å to 20Å

Ultramicropores: less than 10Å.

A brief description of the methods used for pore characterization is given below.

3.1.1 Mercury Porosimetry

This method[32,33] works on the fact that mercury is non wetting on most surfaces and hence has to be forced into pore under pressure. The relation between the pore size and the applied pressure P, is given by the Laplace equation

$$r = -2\gamma \cos(\theta)/P \qquad (3.1)$$

where γ is the interfacial surface energy, θ is the contact angle between the walls of the pore and mercury.

This method is highly automated, can analyze wide pore size ranges (20Å - 20mm), and has high volume resolution. However uncertainty in contact angle and surface tension, inability to probe microporosity, destruction of the sample in

several cases and the need to dry the sample before analysis make it unfavorable for many purposes.

3.1.2 BET Method

This is probably the earliest method for determining the surface area. Langmuir's work relating the volume of the gas adsorbed to the relative pressure p/po was modified by Brunauer, Emmett and Teller (BET)[34] to account for multilayer adsorption, since Langmuir assumed a monolayer adsorption. For BET analysis, the adsorption data (V vs. p/p_o) is plotted in the linear form of the BET equation.

$$\frac{1}{V\left(\frac{p_o}{p}-1\right)} = \frac{1}{V_M C} + \frac{C-1}{V_M C\left(\frac{p}{p_o}\right)} \qquad (3.2)$$

For values of P_o/P in the range 0.05 - 0.3 equation (3.2) is usually linear and the desired monolayer volume V_m and the parameter C can be obtained from the slope and the intercept, respectively. Surface area can then be calculated from a knowledge of the cross-sectional area of the adsorbed molecule. Pore sizes are determined at higher pressures where Kelvin equation is employed. This approach is usually limited for pore size greater than 500Å.

3.1.3 Permeability Data

This is by far the easiest method for characterization of pores. But it lacks

precision and only gives a rough estimate of the pore size. Moreover only those gases that are not adsorbed on the surface can be used here. The pore size[35,36] can be obtained from a knowledge of the permeability coefficient for a particular gas such as He or H_2, which can be obtained as explained earlier. Diffusivity is related to the permeation coefficient according to the equation,

$$D_i = (P_i RT/\varepsilon_M) \qquad (3.3)$$

where P_i is the permeability of the gas, D_i is the diffusivity (cm^2s^{-1}) and ε_M is the porosity of the membrane, which in our case was 0.28 for a virgin vycor tube (provided by the manufacturer). Pore sizes are then obtained from standard plots of $\log_{10}(D)$ against $\log_{10}(d)$, where d is the pore diameter in Angstroms. These plots can be found in literature.

The experiment could be repeated for several non adsorbing gases and an average value for pore size could be obtained. As it is evident from the procedure, this method doesn't require any sophisticated equipment and is less time consuming.

3.1.4 NMR Measurements

NMR is a magnetic spectroscopy that relies on the quantization of the magnetic moments of nuclei in the presence of a magnetic field. NMR is an energy

transition that is very sensitive to the local environments surrounding the nuclei. The property of interest is the relaxation time.

Relaxation time is the time required for the magnetization to reach equilibrium along the magnetic field. It is found that the molecules lying along the pore walls have more mechanisms for relaxation than those in the center and hence have shorter relaxation times. The relaxation time is related to the pore size by the relation,

$$1/T_1 = \alpha + \beta/r_p \qquad (3.4)$$

where α and β are constants and r_p is the hydraulic pore radius.

3.1.5 Gas Adsorption/Desorption

This method[37] has been very successful for polymeric membranes. Pore sizes down to 20Å have been determined. It works on the principle that a hysterisis loop occurs between adsorption and desorption curves when a full isotherm is measured. This has been explained as due to the presence of a concave meniscus in the pores which lowers the vapor pressure of the adsorbate. The lowering of the vapor pressure (p) for a cylindrical capillary of radius r_k is given the equation

$$RT \ln\left(\frac{p}{p_o}\right) = \frac{-2\gamma V_L}{r_k}\cos\theta \qquad (3.5)$$

where p_o is the saturated vapor pressure of the system at temperature T, γ and V_L are the surface energy and molar volume of the adsorbent, and θ is the angle of contact.

Pore radius r_p can then be calculated by the equation

$$r_p = r_k + t \tag{3.6}$$

where t is the thickness of the adsorbed layer of vapor in the pores.

3.2 Mechanisms for Separation

A brief knowledge about the different mechanisms[37] for gas separation in membranes is essential in order to explain the observed phenomenon. The next few pages discuss the various mechanisms available for gaseous separation and the limiting factors under which they operate.

3.2.1. Knudsen Separation

Differences in Knudsen diffusivities[38] of the diffusing species in the pore can lead to separation. According to Knudsen, separation is possible if the mean free path of the gas molecules is greater than the mean pore diameter. The mean free path is related to the molecular diameter, d_m of the gas by the equation

$$\lambda = \frac{1}{\sqrt{2}c\pi d_m^2} \tag{3.7}$$

where c_i is the molar concentration.

In the Knudsen regime, the flow of a gas depends on its molecular weight and is related according to the equation

$$q_k = \left(\frac{32\pi}{9MRT}\right)^{1/2} \frac{R^3 \Delta P}{\delta} \qquad (3.8)$$

where, R is the pore radius, ΔP is the pressure differential across the membrane, δ is the equivalent thickness of the membrane, M is the molecular weight of the gas and q_K is the flux of atoms/molecules through the pore.

So at a given temperature and for a certain pore diameter the ratio of diffusivities D_A and D_B, of gases A and B respectively, would be

$$D_A/D_B = \sqrt{[M_A / M_B]} \qquad (3.9)$$

This is the major mode of transport in microporous membranes with pore sizes ≥40Å but less than 100Å. At temperatures greater than 325°C and pressures less than 2 atm, the total flow approaches Knudesn diffusion[39]. The separation obtained by this method is the least of all cases.

3.2.2 Molecular Sieving

Molecular[40] sieving involves selectively allowing the gas molecules based on

their radii. It is quite evident that for separation by this mechanism, the pore sizes should lie somewhere in between the molecular radii of the two gas molecules. The efficacy of separation is greater if the difference in molecular radii is larger. A list of atomic radii is given below to have a better understanding of the pore sizes needed for this mechanism to operate.

Table 3.1 Atomic Radii

Gas	He	H_2	Ar	N_2	CH_4
Radii(Å)	2.15	2.70	3.58	3.70	4.14

From the table, we can conclude that the pore size has to be between 2.70Å to 3.50Å for separation of H_2 from N_2. It is to be appreciated here that since the difference in radii is very small, the pore size distribution has to be very narrow. This mechanism is used in several nanoporous carbon membranes[35].

3.2.3 Capillary Condensation and Multilayer Diffusion

In this case, gas molecules are selectively adsorbed or condensed[41,42] in the pores and then diffused through the condensed liquid. Very high permeabilities are obtained here, since multilayer diffusion is faster than diffusion in air or gas. This is the dominating mechanism in polymeric membranes[43] and hence have high permeabilities compared to ceramic membranes. This mechanism can be explained by Kelvin's Equation.

The occurrence of multilayer diffusion and capillary condensation is mainly dependent on the relative pressure of the vapor, whereas the relative pressure is dependent on temperature and pressure. A third variable is the mean pore size of the membrane. Smaller pore sizes will give rise to lower relative pressures. Two models which explain multilayer diffusion are the hydrodynamic model and the hopping model. The first model considers the multilayer flux as a two-dimensional fluid, slipping over the surface. The second model considers flux by jumps of adsorbed molecules from site to site. A case of capillary condensation occurs when the thickness of the adsorbed multilayers equals the pore radius.

The adsorption of organic molecules is more favorable compared to inorganic gas molecules because of their low vapor pressure[5]. This forms the major difference from the earlier two mechanisms. The permeability of organic molecules, which have higher mass and larger radii, is higher than the inorganic molecules. The permeability of inorganic molecules in the presence of organic molecules is almost zero since the pores are fully clogged by the condensed liquid and also due to the fact that these molecules are not readily soluble in the condense.

Asaeda et al[41] employed this technique to separate water from alcohol, with water being the preferentially permeating component. The multilayer diffusional flux is much larger than the gas phase flux.

Aseada *et al*[41] employed this technique to separate water from alcohol, with water being the preferentially permeating compound. The multilayer diffusional flux is much larger than the gas phase flux.

3.2.4 Configurational Diffusion

It has long been known that as the pore size decreases, the effects of molecule-wall collisions increase, and the flux tends to decrease. In this case Knudsen diffusion cannot explain the transport phenomenon, because of its assumption that molecule-pore wall interactions are negligible.

Configurational diffusion[42] is a relatively new model introduced to explain the transport properties in pores with molecular dimensions. According to Bird *etal*[48]. there exists a kind of layer close to the walls in which the molecule-wall interaction is not simple collision. The heavier molecules remain in the layer for a longer time and will collide with the walls more frequently than the smaller molecules. This situation gives rise to segregation in the fluxes of molecules with different radii. In this regime, diffusion depends on the size and configurational structure of molecules. Configurational structure includes the dynamics of rotations and vibrations of the different groups in the molecule. Thus, there is a difference of two orders of magnitude between the diffusivities of *cis*- and *trans*-butene molecules. Configurational diffusion is flanked on one side by Knudsen diffusion and on the other probably by molecular sieving. Fig 3-1 shows the

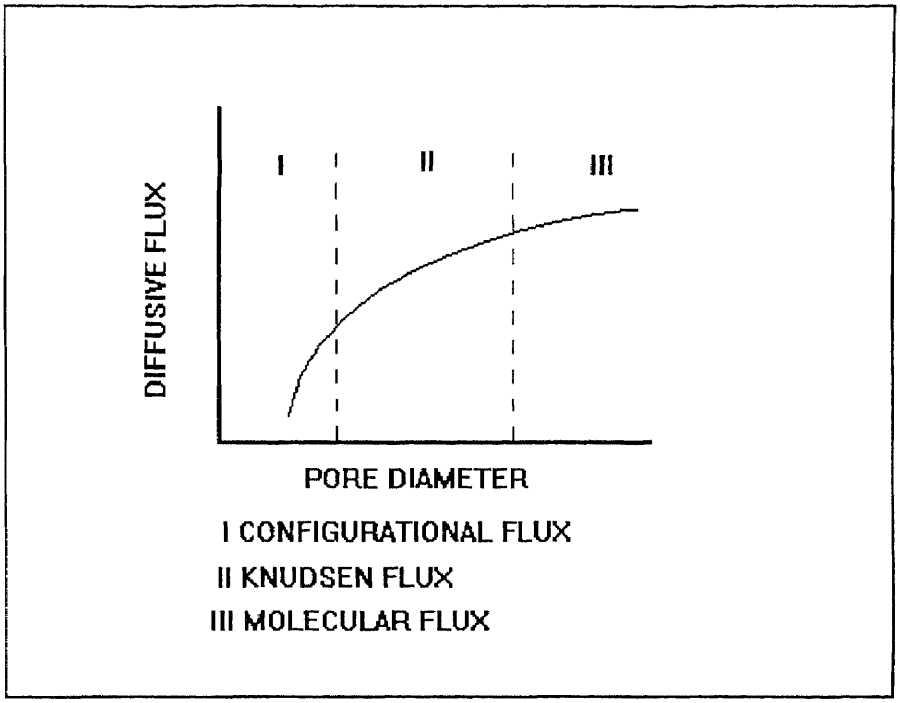

Figure 3-1 Type of diffusion regime as a function of the pore diameter

CHAPTER 4

EXPERIMENTAL PROCEDURES

4.1 Setup of the Apparatus

A schematic diagram of the apparatus is shown in figure 4-1. It consists of a 3-zone horizontal reactor made of fused quartz with an inner diameter of 13.5 cm and a length of 144 cm. The reactor is heated by resistance elements wound around it. Heat transfer takes place by convection. One end of the reactor is connected to a vacuum system, while the other end is provided with a door along with a vent for inserting the vycor tube. The vacuum system consists of a dual stage rotary vane pump and a roots blower. The pressure in the system was monitored by standard MKS baratron gauges, while it was also controlled through the use of a butterfly valve. Together the system could maintain a base pressure of about 30 mTorr. The reactor had a peak pressure limit of 760 Torr and hence all the measurements were carried out below atmospheric pressure. Also, the reactor had an effective temperature control range from 200°C to 1400°C. However, in our study the maximum temperature reached was less than 500°C. This care was taken to prevent any undesirable sintering of the porous vycor tube into a non-porous tube.

Stainless steel tubing's were used to deliver the reactants and the permeate gases into the reactor. The setup was made leak proof by using Cajon

fittings and O-rings, wherever necessary. TEAB was injected into the reactor using a gas bubbler, but in the opposite sense of its actual function. Nitrogen gas was introduced through the outlet port at a pressure of 6psi while TEAB was forced out through the inlet port. TEAB was subsequently carried through a capillary tube into the reactor.

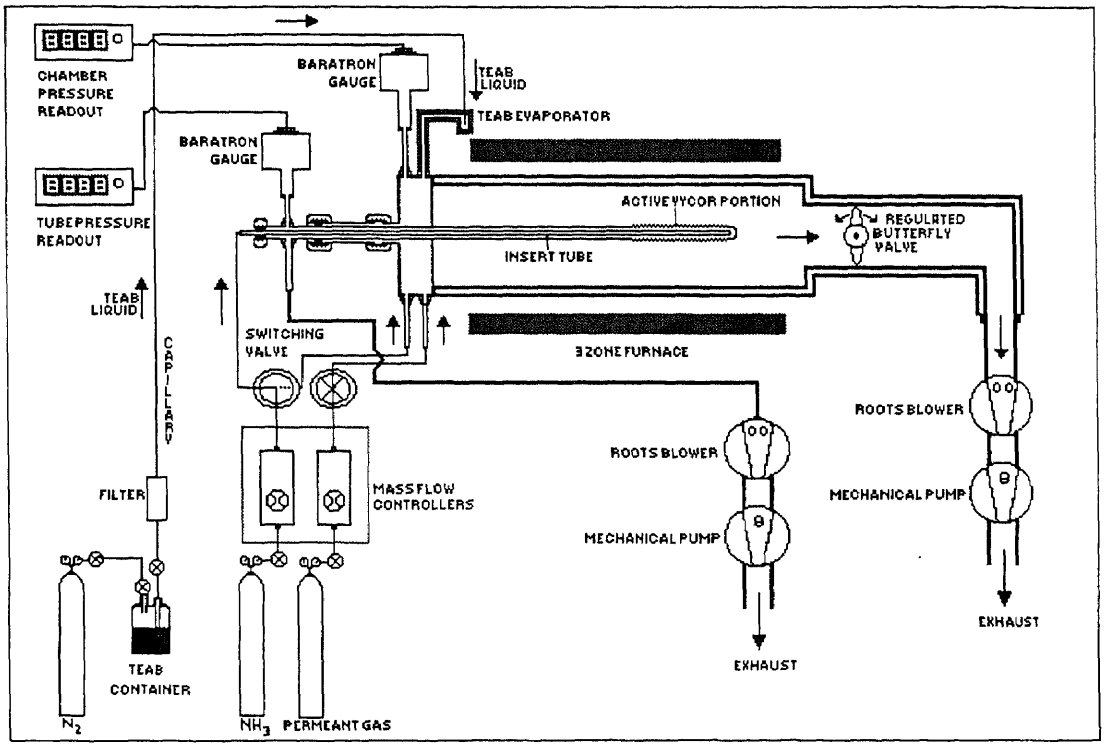

Figure 4-1: Apparatus setup for the synthesis of BN membranes

4.2 BN Deposition

Once the equipment was ready for deposition, the reactor was gradually heated up to the desired temperature following a steady rate of 150°C/Hr. The reactor was then pumped overnight to get rid of degassing from the vycor tube and the

walls of the reactor. Sufficient time was allowed for the rate of degassing to fall below 3mTorr/min. Degassing was checked regularly by closing all the valves leading to the reactor and monitoring the rate of increase in pressure inside the reactor.

The reactants were then introduced into the chamber. TEAB lines were heated up to 80°C-100°C to vaporize the liquid before it enters the chamber. After a predetermined time of deposition had elapsed, the deposition was ceased by closing all the inlet valves and pumping down the chamber. The reactor was again pumped overnight before permeability measurements could be carried out.

4.3 Permeability Measurement

Permeability can be roughly defined as the ease with which a gas can pass through the open pores of the membrane. As has already been discussed the mode of permeation depends on the interaction between the permeate molecules and the walls surrounding the pores. Transport properties can be determined by studying the pure gas permeability behavior of the membrane

Individual gas permeability study is done to find the permeability coefficient of a gas. The main drawback is that it does not show the interaction effects due to the presence of other gases. Here permeate is fed at high pressure into the chamber (max. 400 Torr) while a very low pressure is maintained in the tube. This pressure differential causes the gas molecules

such as He, H_2 and N_2 to permeate through the membrane into the tube. This results in the increase in the pressure inside the tube, when the tube is isolated from the vacuum system. The rise of pressure is noted with time. It is assumed

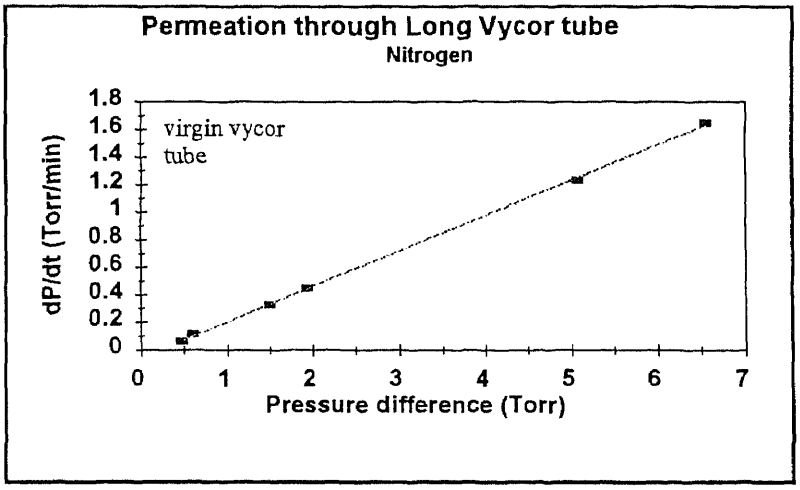

Figure 4-2 Method of estimating permeability coefficient

that there is no appreciable drop in the pressure outside the tube which can affect our data. A plot of rate of pressure rise with respect to the pressure differential is plotted in figure 4-2. As can be seen the plot yields a straight line and the slope of this line is proportional to the permeability coefficient. The proportionality constant is the standardised volume of the vycor tube. The volume estimated for the experimental vycor tube which had a length of 63.5cm and an inner diameter of 0.518cm was 13.38cm^3.

CHAPTER 5

RESULTS AND DISCUSSION

Before going any further, it is reiterated here that the setup of the apparatus and some of the deposition conditions were similar to an earlier project dealing with BN thin films. Hence the calibration for the flow of TEAB through the capillary has been used directly from this project.

5.1 Virgin Vycor Tube Measurements

Permeability measurements were carried out on virgin Vycor tube before deposition. In figure 5-1, the permeation coefficient is plotted as a function of inverse square root of the molecular weight of the permeate gases. The figure

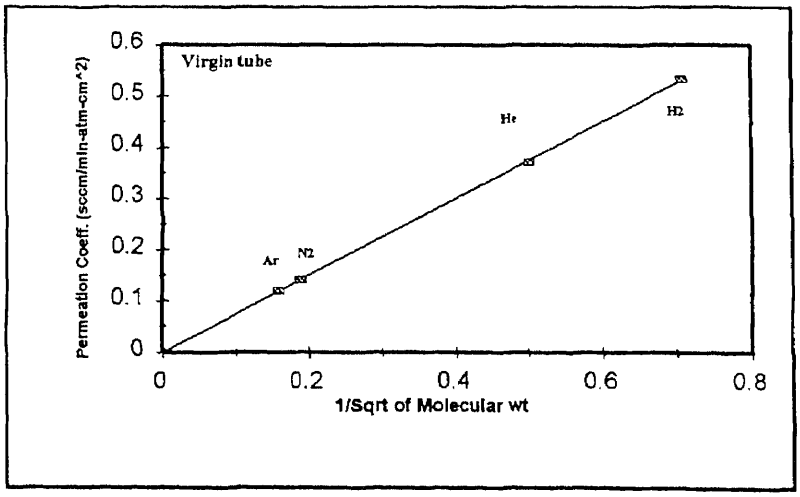

Figure 5-1 Permeability value-Molecular weight relationship of various gases for a virgin vycor tube at 300°C

shows that the permeability values are linearly related to the inverse square root of the molecular weight. This proves that the transport properties are fundamentally dominated by Knudsen diffusion, which was expected since the mean pore size was about 40Å. The same behavior was observed when the temperature was varied. The results also confirm that the vycor tube is void of any defects, since the presence of cracks would indicate diffusion by molecular flux mechanism. It is of utmost importance to be assured that the vycor tube is free of cracks or pinholes since the data obtained on subsequent deposition could be quite erroneous.

5.2 Deposition at 475°C

Boron Nitride was deposited at different temperatures and at different NH_3 pressures. Throughout the experiment the flow of TEAB and the pressure inside

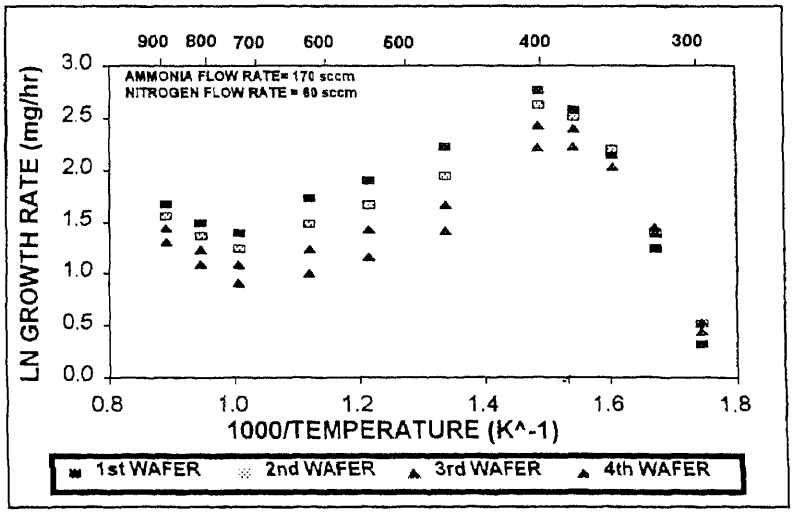

Figure 5-2 Temperature-growth rate relationship for depositing BN thin films on Si wafers

the reactor was maintained steady at 17sccm and 0.5 Torr respectively, which was determined to be reasonable for depositing thin films in our reactor. Figure 5-2 shows the trend in variation of growth rate[47] of BN on Si wafer against temperature as a variant.

Initial deposition was carried out at 475°C using same-side reactants geometry. Both TEAB and NH_3 were introduced by separate lines into the reactor while maintaining vacuum inside the vycor tube. The results are shown in figure 5-3 which gives the drop of permeability of He, N_2 and Ar with deposition

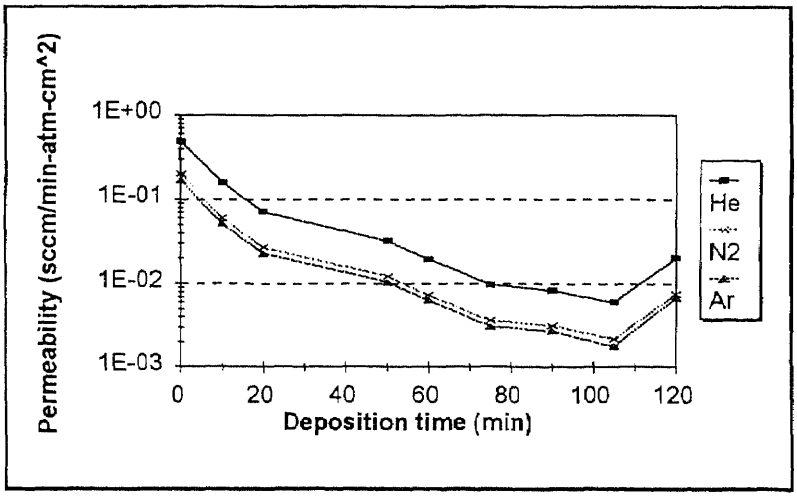

Figure 5-3 Drop in permeability values of inorganic gases with deposition time for membranes obtained at 475°C using same side reactant geometry

time. The foremost observation is that there is a drop in permeability with increasing deposition time. This implies that the resistance to the flow of gases through the vycor tube increased due to deposition of BN. However, the rate of drop of permeability for each gas is the same and thus no effective increase in

separation factor was observed, apart from the initial Knudsen separation. The most probable reason for such a behavior is that the BN layer could contain a large number of pinhole defects, but with a porosity less than the virgin vycor tube. The presence of pin holes could be explained by taking into factor high deposition temperature and the probability of occurrence of gas phase. As was

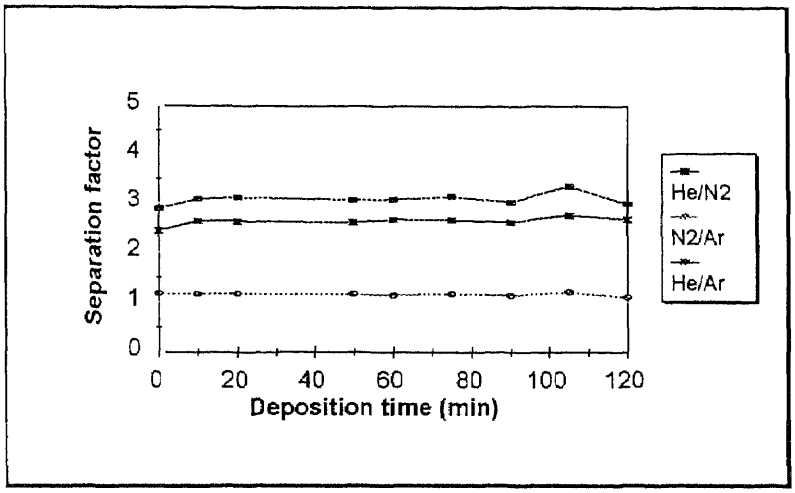

Figure 5-4 Variation of separation factor for various gases with deposition time for a membrane obtained at 475°C using same-side reactant geometry

explained earlier, gas phase nucleation resulted in particulate deposit and enhanced the formation of pinholes. Figure 5-4 shows the change in separation factor with increasing deposition time. From fig.5-4 it is apparent that, though there is a drop in permeability, separation is still effected through Knudsen diffusion.

BN was then deposited using opposite-reactants geometry, which is reported to yield better results[44]. TEAB was passed outside the Vycor tube while

NH_3 was passed inside the vycor tube. This configuration was conducive for *in-situ* permeability measurements. In this case, the drop in permeabilities was much rapid than in the earlier case. Still, the rate of drop was similar for all the gases and hence no further improvement in separation was observed. The reason for such a behavior is believed to be similar to the previous experiment.

Also, both the experiments revealed that the permeabilities of the gases increased after a sufficient long deposition had occurred. This was possibly due to the formation of cracks in the layer. Cracks are believed to be initiated due the development of stress in the deposit. As more and more material is deposited, the film stress increases, thus opening up the cracks that had been initiated. According to Paturi[47], BN thin films deposited on Si wafers had tensile stresses in the temperature range of 350°C to 475°C, while compressive stresses prevailed below 325°C. Though, the stress conditions are entirely different on a curved surface, as in the case of porous membranes, when compared to flat surfaces, to a first approximation it is reasonable to deduce the type of stresses that can prevail in porous membranes based on film stress on flat surfaces. To overcome the problem of stresses and gas phase nucleation, deposition was then carried out at lower temperatures. Boron nitride was deposited at 300°C and 250°C. The chamber pressure was again maintained at 0.5 Torr with a TEAB flow rate of 17sccm.

5.2 Deposition at 300°C

The results for deposition at 300°C are shown in fig 5-5, which gives the decrease in permeability with deposition time. As before there is an appreciable drop in permeability with deposition time. Interestingly, the rate of drop is substantially different for different gases. Larger molecules face more resistance to permeation than smaller gases. The percentage drop in permeability for lighter gases such as He and H_2 is much lower than for the heavier gases. The transport of heavier gases, such as N_2 and Ar, is now restricted to the larger

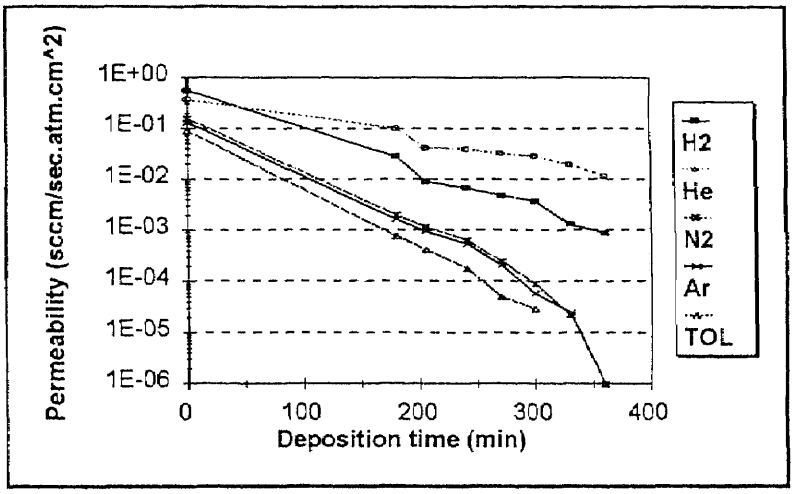

Figure 5-5 Permeability drop of various gases with deposition time for membranes obtained at 300°C

pores which are still large enough to allow larger molecules to diffuse under knudsen regime. Hence they still obey the knudsen equation as can be inferred from figure 5-7. The lighter molecules such as He and H_2 can diffuse through both the larger and the smaller pores. However, due to the large percentage of

smaller pores resulting from a narrow pore size distribution, the contribution to total flux by the larger pores is negligible. Hence, smaller molecules do not show Knudsen behavior even though some of them permeate through the larger pores.

Here, the permeability characteristics of toluene gas were also studied. After a total deposition time of 6 hours, no detectable amount of toluene was observed in the permeate side. This is an indication that the pore size is now down to a level where it selectively blocks off toluene. Figure 5-6 shows the increase in separation factor with deposition time at 300°C.

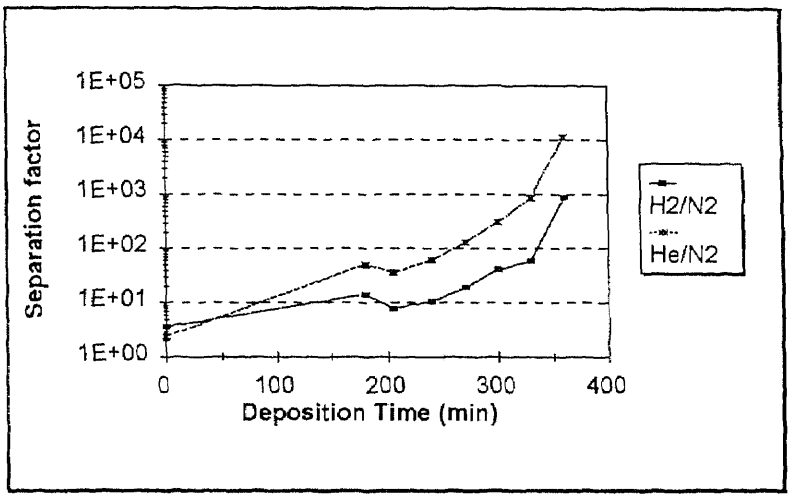

Figure 5-6 Variation of separation factor of inorganic with deposition time for membranes obtained at 300°C

The membranes obtained at 300°C showed some peeling effect when it was exposed to atmosphere. It can indicate bad adhesion of BN to the vycor tube or small depth of penetration of TEAB into the pores.

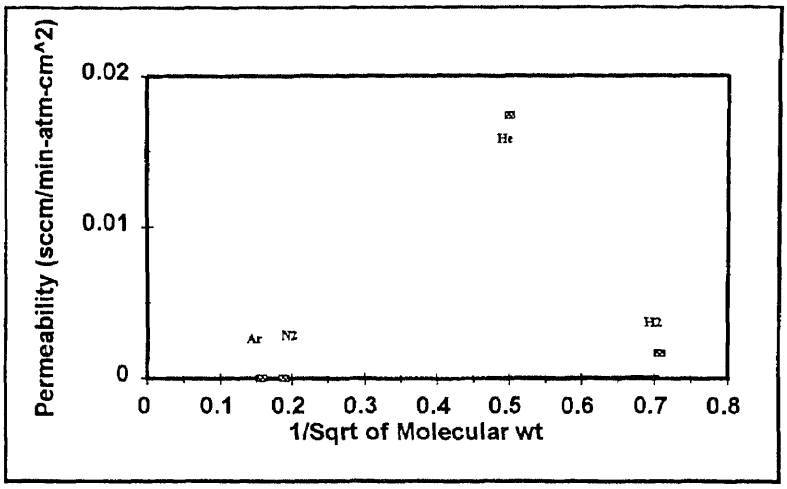

Figure 5-7 Deviation of smaller molecules from Knudsen behavior for a membrane obtained at 300°C

5-3 Deposition at 250°C

BN was also deposited at 250°C to study the effect of temperature on the rate of drop of permeability. Figure 5-8 shows that a separation factor of 11000 for

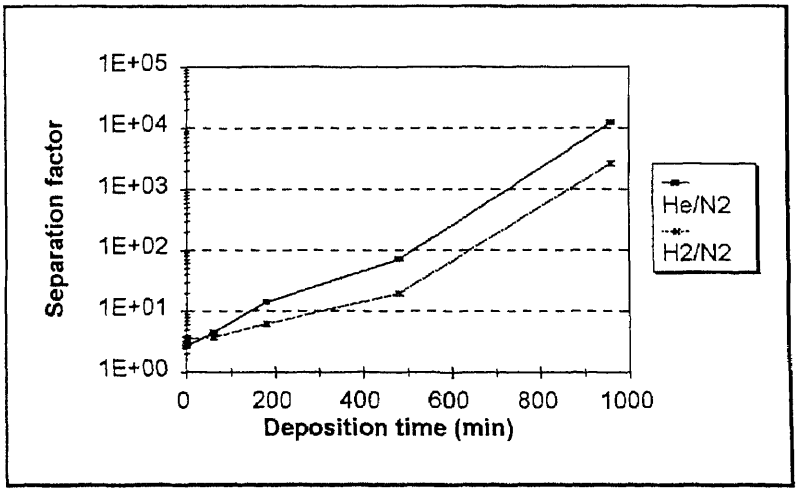

Figure 5-8 Variation of separation factor for various gases for a membrane obtained at 250°C

He/N_2 could be achieved in 16 hours, which is much longer than the time required for the same separation factor at 300°C. This is confirmation of the fact that the deposition rate decreases with temperature, thus leading to slower plugging of pores in the membrane. However, no cracks were observed during or after deposition and even when exposed to air for a long period.

5.5 Activation Energy

Activation energy study was done by measuring the change in the permeabilitiy values of the gases at different temperatures. For this study, the membrane was synthesized at 300°C for 6 hours. Permeability was measured at 250°C, 300°C, 325°C, and 350°C. The permeability values have been modified so that only the effect of BN deposit could be studied. The total flux of the membrane, Q is given by

$$\frac{1}{Q} = \frac{1}{Q_t} + \frac{1}{Q_f} \tag{5.1}$$

where Q_t and Q_f are the gas flux contributions of the virgin vycor tube and of the BN film respectively. Since, the values of Q_t and Q are measured, the value of Q_f could be determined from the above equation.

A semilog plot of permeabilitiy coefficients against the inverse of absolute temperature yielded linear relationship as shown in figure 5-9 for He and H_2, and in figure 5-10 for N_2. It is clear from the exponential behavior of the

permeabilities, the transport of He and H_2 follow Arrhenius behavior and hence are thermally activated. However, permeability of N_2 exhibits a totally different

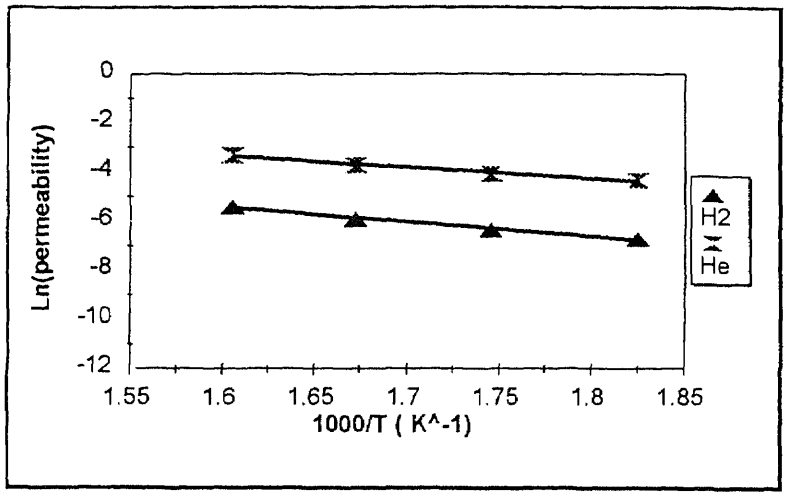

Figure 5-9 Arrhenius behavior of gas permeation exhibited by smaller molecules for a membrane obtained at 300°C

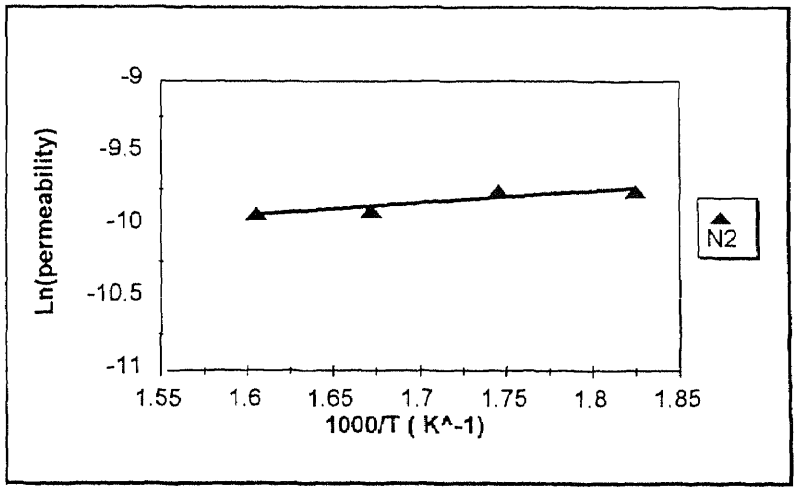

Figure 5-10 Temperature-permeability relationship for larger molecules such as N_2 in accordance with Knudsen diffusion

behavior and is not thermally activated. Permeabilities of N_2 decrease with increase in temperature. This could indicate that N_2 molecules still obey Knudsen equation (eqn 3.8), probably due to the presence of residual microporosity or pinholes. Similar results have been reported by Megiris[44] et al. The activation energies from the slope are 40 kJ/mol for He and 50 kJ/mol for H_2. These values are very high compared to those reported in literature[44,45] because of the extremely small size of the pores.

5.6 Stability of the Membrane

Stability of the membranes has been assessed by two methods: Thermal stability[46] and environmental stability. Thermal stability was carried out in-situ during permeability measurements at different temperatures. The results showed that membranes obtained at 300°C were in excellent condition as long as the temperature was maintained at 300°C. But, when the membranes were subjected to activation energy studies, cracks developed at temperatures in excess of 350°C. This was noted by observing the sudden increase in the permeability values of all the gases. Cracks could be clearly seen in an electron microscope as well as in optical microscope. Another reason could be that at these high temperatures, sintering could take place and thus increase the pore size. These membranes were then placed in atmosphere to further evaluate the effect of moisture on the structural integrity of the deposits. After a few days, it

was found that the deposit started to peel off from the support indicating lack of enough adhesion.

The same procedure was carried out for membranes obtained at 250°C. No significant changes were observed in the permeability values even after going through a thermal cycle. The membranes stayed intact and no cracks were observed. Again, in atmospheric conditions no further damage was observed.

CHAPTER 6

CONCLUSIONS

The synthesis and characterization of BN membranes using TEAB and NH_3 as precursors has been investigated. BN was deposited on mesoporous vycor tubes at different temperatures and by different deposition geometries. Membranes obtained using counter reactants geometry yielded more favorable results than same-side reactants geometry. Also, higher deposition temperatures did not result in an increase in separation factors beyond the Knudsen value. Lower deposition temperatures gave excellent separation factors. At 300°C, He/N_2 and H_2/N_2 permeability ratios were close to 11,000 and 1000 respectively. However, no separation was observed between N_2 and Toluene. Also, the membranes were rather weak and exhibited peeling behavior when exposed to atmosphere. Membranes obtained at 250°C also had high separation factors, but longer deposition time was required. Once again, no separation between N_2 and toluene was achieved. The membranes were very stable and showed no cracks or peeling under atmospheric conditions. XRD analysis indicated that the BN deposit was amorphous.

There is additional work to be done in this field. Future research is aimed at enhancing the deposition rate and in investigating the effect of gaseous mixtures on the separation factors. More importantly, the separation of VOC's from inorganic gases will be given more attention.

REFERENCES

1. Chan K.K.; Brownstein A.M. *Ceram Bull.* **1991**, 70, 703.
2. Kajiwara M. *Sepn. Sci. & Tech.* **1991**, 26, 841.
3. Feng, X.; Sourirajan, S; Tezel, F. *Ind. Eng. Chem. Res.* **1993**, 32, 533.
4. Hsieh H.P.; Liu P.K.T.; Dillman T.R. *Polymer J.* **1991**, 23, 407.
5. Uhlhorn R.J.R.; Keizer K.; Burggraaf A.J. *J. Membr. Sci.* **1992**, 79, 259.
6. Zanetti, R. *Chem. Engg.* June 9 **1986**, 19.
7. Haggin, J. *C&EN,* June 6 **1988**, 7.
8. Wu, J.C.S.; Liu P.K.T. *Ind. Eng. Chem. Res.* **1992**, 31, 322.
9. Tonkovich, A.L.Y.; Secker, R.B.; Cox, J.L. *Sepn. Sci. & Tech.* **1995**, 30, 1609.
10. Neureither B.; Basa, C.; Blumenstock, K. *J. Electrochem. Soc.* **1993**, 140, 3607.
11. Hamilton, E.J.M.; Dolan, S.E.; Mann, C.M. *Sci.* April **1993**, 260, 659.
12. Baskaran S.; Halloran J.W. *J. Am. Ceram. Soc.* **1994**, 77, 1249.
13. Shelekhin, A.B.; Dixon, A.G.; Ma, Y.H.; "A Theory of Gas Diffusion and Permeation in Molecular-Sieve Membranes", MS Thesis, Worcester Polytechnic Institute, Worcester, MA. **1991**.
14. Rand, M.J.; Roberts J.F. *J. Electrochem. Soc.* **1968**, 15, 423.
15. Baronian, W. *Mater. Res. Bull.* **1972,** 7, 119.
16. Nakamura, J. *J. Electrochem. Soc.* **1986**, 133, 1120.
17. Nakamura J. *J. Electrochem. Soc.* **1985**, 132, 1757.
18. Heitsch C.W. *Inorg. Chem. Hand.* **1965**, 4, 1019.

19. Xu, Q.; Anderson, M.A. *J. Mater. Res.* May **1991**, 6, 1073.

20. Peterson; Webster E.T.; Hill Jr. C.G. *Sepn. Sci. & Tech.* **1995**,30, 1689.

21. Trocha M.; Koros W.J. *J. Membr. Sci.* **1994**, 95, 259.

22. Collins, J.P.; Way, J.D. *Ind. Eng. Chem. Res.* **1993**, 32, 3006.

23. Hsieh, H.P. *AIChE Symposium series **1991*** 84, 1.

24. Turner, W.E.S.; Winks, F. *J. Soc. Glass. Tech.* **1926,** 10, 102.

25. Abe, T. *J. Amer. Ceram. Soc.* **1952**, 35, 284.

26. Ohring, M. *In The Materials Science of Thin Films* Academic Press, Harcourt Brace Jovanovich Publis. NY. **1992**.

27. Vekita, M.; Nelson, K.F.; Bates Jr. W. *Thin Solid Films* **1982**,88, 275.

28. Boone, J.I.; Van Doren, T.P.; Berry, A.K. *Thin Solid Films* **1982**, 87, 259.

29. Lin Y.S.; Burggraaf. A.J. *AIChE Journal* **1992**, 38, 445.

30. Smith D.M.; Hua, D.; Earl, W.L. *MRS Bull.* April **1994**, 44.

31. Bottino. A.; Capannelli, G.; Petit-Bon, P. *Sepn. Sci. & Tech.* **1991**, 1315.

32. Rocek J.; Uchytil P. *J. Membr. Sci.* **1994,** 89, 119.

33. Mikulasek, P.; Dolecek, P. *Sepn. Sci. & Tech.* **1994**, 29, 1183.

34. Smith, D.M.; Hua D-W.; Earl, W.L.; *MRS Bull.* April **1994**, 44.

35. Rao, M.B.; Sircar, S. *J. Membr. Sci.* **1993**, 85, 253.

36. Yasuda. H.; Tsai.J.T. *J. Appl. Poly. Sci.* 97, 805.

37. Smolders. C.A. *J. Membr. Sci.* **1992**, 73, 259.

38. Uhlhorn R.J.R.; Keizer K.;Vuren R.J.; Burggraaf A.J. *J. Membr. Sci.* **1988**, 39, 285.

39. Wu J.C.S.; Flowers D.F.; Liu P.K.T. *J. Membr. Sci.* **1993,** 77, 85.

40. Klein, L.C.; Gizspenc, N. *Ceram. Bull.* **1990**, 69, 1821.

41. Asaeda M.; Du L.D. *J. Chem. Eng. Jpn.***1986,** 19, 72.

42. Cunningham R.E.; Williams R.J.J. *In Diffusion in Gases and Porous Media,* Plenum Press, NY, **1980**.

43. Peterson E.S.; Stone M.L.; McCaffery R.R.; Cummings D.G. *Sepn. Sci. & Tech.* **1993,** 28, 423.

44. Megiris, C.E.; Glezer, H.E. *Ind. Eng. Chem. Res.*,**1992**, 31, 1293.

45. Tsapatis, M.; Kim, S.; Nam, S.W. *Ind. Eng. Chem. Res.* **1991**, 30, 2152.

46. Lin, Y.S.; Chang, C.; Gopalan, R. *Ind. Eng. Chem. Res.* **1994**, 33, 860.

47. Paturi V."Synthesis and Charac. of BN Thin Films for X-ray Masks", MS Thesis, New Jersey Institute of Technology, Newark, NJ, **1991**

48. Bird, R.B.; Stewart, W.E.; Lightfoot, E.N. *In Transport Phenomenon,* John Wiley & Sons, NY, **1960.**